Contents lists available at ScienceDirect

Infectious Disease Modelling

On optimal control at the onset of a new viral outbreak☆,☆☆

Alexandra Smirnova *, Xiaojing Ye

Department of Mathematics & Statistics, Georgia State University, Atlanta, USA

A B S T R A C T

We propose a versatile model with a flexible choice of control for an early-pandemic outbreak prevention when vaccine/drug is not yet available. At that stage, control is often limited to non-medical interventions like social distancing and other behavioral changes. For the SIR optimal control problem, we show that the running cost of control satisfying mild, practically justified conditions generates an optimal strategy, $u(t)$, $t \in [0, T]$, that is sustainable up until some moment $\tau \in [0, T)$. However, for any $t \in [\tau, T]$, the function $u(t)$ will decline as t approaches T, which may cause the number of newly infected people to increase. So, the window from 0 to τ is the time for public health officials to prepare alternative mitigation measures, such as vaccines, testing, antiviral medications, and others. In addition to theoretical study, we develop a fast and stable computational method for solving the proposed optimal control problem. The efficiency of the new method is illustrated with numerical examples of optimal control trajectories for various cost functions and weights. Simulation results provide a comprehensive demonstration of the effects of control on the epidemic spread and mitigation expenses, which can serve as invaluable references for public health officials.

1. Introduction

The circulation of infectious diseases, such as COVID-19, is shaped by multiple parameters including control interventions (Perkins & España, 2020), environmental factors (Weiss & McMichael, 2004), immunity patterns (O'Driscoll et al., 2021), superspreading events (Lloyd-Smith, Schreiber, Kopp, & Getz, 2005), and behavior changes (Radin et al., 2021). These factors impact the early growth dynamics (Szendroi & Csanyi, 2004) and the basic reproduction number (Locatelli, Trächsel, & Rousson, 2021), which quantifies the number of secondary cases per primary case in a completely susceptible population.

Since the first COVID-19 case was detected in December 2019, the disease spread rapidly causing a worldwide pandemic. While some infected people experience only mild or moderate symptoms, others can get seriously ill and require immediate medical intervention (Drugs.com, 2022; Li et al., 2020; Tang et al., 2020; Zhao et al., 2020). Among high risk individuals are elderly people and those with underlying health conditions such as cancer, diabetes, chronic respiratory disease, and others (CDC Center for Disease Control and Prevention, 2023a). As of April 14, 2024, there have been 775,335,916 confirmed cases of

COVID-19, including 7,045,569 deaths (WHO World Health Organization, 2023). Important factors contributing to the alarming rise in COVID-19 cases at the early stage of the pandemic were high reproduction number, a large number of "silent spreaders" (especially among young people), and a relatively long incubation period (CDC Center for Disease Control and Prevention, 2023b). In the absence of vaccines and antiviral treatments in late 2019 and early 2020 (HHS U.S. Department of Health and Human Services, 2023), mitigation measures such as social distancing (including full or partial lockdowns), restrictions on travel and mass gatherings, isolation and quarantine of confirmed cases, change from in-person to online education, and other similar tools emerged as the key ways of control and prevention (Organisation for Economic Co-operation and Development, 2023; Summer, Aghaee, Martcheva, & Hager, 2023). While these measures proved to be effective in a short-term, they are hard to sustain in a long run due to their negative impact on mental health coupled with high social and economic cost. Hence, since the start of COVID-19, balancing pros and cons of early non-medical interventions has come to the forefront (not only to contain COVID-19, but also to prepare for future epidemic outbreaks) (David Paltiel, Zheng, & Walensky, 2020; Hadi & Ali, 2020; Igoe et al., 2023; Lee, Chowell, & Castillo-Chávez, 2010; Marshall, Barlow, & Tyson, 2021; Pal Bajiya, Bugalia, Tripathi, & Martcheva, 2022; Panovska-Griffiths et al., 2020; Pazos & Felicioni, 2020; Pei et al., 2022; Saha et al., 2020, 2022; Saha & Samanta, 2021; Soledad Aronna, Guglielmi, & Moschen, 2020; Svoboda, Tkadlec, Pavlogiannis, Chatterjee, & Nowak, 2022; Tuncer, Timsina, Nuno, Chowell, & Martcheva, 2022; Vincent et al., 2022).

In this paper, we consider an optimal control problem for SIR compartmental model (Susceptible → Infectious → Removed) of early disease transmission. We design a running cost of control with mild, practically justified conditions that give rise to the optimal control strategy, $u(t)$, which does not exceed its admissible upper bound for the entire duration of the study period, $[0, T]$. Our theoretical analysis indicates that at the early stage of an outbreak, the optimal control strategy, $u(t)$, may be growing until some moment $\tau \in [0, T]$. However, for any $t \in [\tau, T]$, the function $u(t)$ will decline as t approaches T, which may cause the number of newly infected people to increase. So, the window from 0 to τ is the time for public health officials to prepare alternative mitigation measures, such as vaccines, testing, antiviral medications, and others. Our theoretical findings are illustrated with important numerical examples showing optimal control trajectories for various cost parameters. To learn the optimal control function $u(t)$, we employed a deep learning based numerical algorithm, where $u(t)$ is parameterized as a deep neural network (DNN). The implementation, training and testing of all methods were conducted in Python 3.9.6 with PyTorch 2.1.0 and Torchdiffeq 0.2.3.

2. A strategy for early intervention

At the onset of an emerging epidemic, in the absence of a vaccine and antivirals (HHS U.S. Department of Health and Human Services, 2023; Saha, Samanta, & Nieto, 2018; Saha & Samanta, 2022; Samanta & Gómez Aíza, 2015), the transmission of individuals between different stages of infection is often described by a classical SIR (Susceptible → Infectious → Removed) compartmental model (Dutta, Samanta, & Nieto, 2024; Kudryashov, Chmykhov, & Vigdorowitsch, 2021; Ogilvy Kermack & McKendrick, 1927). For this early and relatively short phase, it is reasonable to infer that natural birth and death balance one another and, therefore, can be omitted. With the disease death rate varying between age and risk groups and being hard to estimate early on, the removed class is assumed to combine recovered and deceased people. Finally, due to the fast dynamic of the initial pre-vaccination stage, we suppose that recovered individuals develop at least a short-term immunity and don't move back to the susceptible class until the end of the study period. Under these assumptions, the SIR (Susceptible → Infectious → Removed/*Immune + Deceased*) model is given by the following system of ordinary differential equations:

$$\frac{d\mathcal{S}}{dt} = -\beta \frac{\mathcal{S}(t)\mathcal{I}(t)}{N} \quad \frac{d\mathcal{I}}{dt} = \beta \frac{\mathcal{S}(t)\mathcal{I}(t)}{N} - \gamma \mathcal{I}(t) \quad \frac{d\mathcal{R}}{dt} = \gamma \mathcal{I}(t) \tag{2.1}$$

The primary goal of our study is to look at possible control strategies that can be effectively introduced at the early ascending stage of an outbreak before more robust mitigation measures, such as vaccines and viral medications, become available. The most common early mitigation measures, which were broadly used during the recent COVID-19 pandemic, include physical distancing, enhanced personal hygiene, mask wearing, awareness, and others. Their primary goal is to "flatten the curve", that is, to reduce the daily number of new infections and, as the result, to reduce the number of virus-related deaths. The SIR model with enforced control, $u = u(t)$, and normalized dependent variables, $S(t) := \frac{\mathcal{S}(t)}{N}$, $I(t) := \frac{\mathcal{I}(t)}{N}$, and $R(t) := \frac{\mathcal{R}(t)}{N}$, takes the form $\frac{d\mathbf{x}}{dt} = f(\mathbf{x}, u)$, where

$$\begin{aligned} f_1(\mathbf{x}, u) &:= -\beta(1 - u(t))S(t)I(t) \\ f_2(\mathbf{x}, u) &:= \beta(1 - u(t))S(t)I(t) - \gamma I(t) \\ f_3(\mathbf{x}, u) &:= \gamma I(t), \end{aligned} \tag{2.2}$$

and $\mathbf{x} = [S, I, R]^\top$. In the above, the admissible set for the control function, $u = u(t)$, is assumed to be

$$\mathcal{U} = \left\{ u \in \mathcal{L}^1[0, T], \quad 0 \leq u(t) < 1 \right\}.$$

In Lemma 2.1 below we show that following the introduction of a time-dependent transmission rate, $\beta(t) := \beta(1 - u(t))$, the model $\frac{d\mathbf{x}}{dt} = f(\mathbf{x}, u)$ remains correct in the sense that the trajectories $(S(t), I(t), R(t))$ starting in a positive octant do not leave the octant and are defined for all $t > 0$.

Lemma 2.1. *Let $u(t)$ be an admissible control trajectory with $\mathbf{x}(t)$ satisfying $\frac{d\mathbf{x}}{dt} = f(\mathbf{x}, u)$ defined in (2.2) and*

$$(S(0), I(0), R(0)) \in \Delta^2 := \{(z_1, z_2, z_3) \in \mathbb{R}^3 : z_1 + z_2 + z_3 = 1, \ z_1, z_2, z_3 \geq 0\},$$

the probability simplex in $\mathbb{R}^3$. Then $(S(t), I(t), R(t)) \in \Delta^2$ for all $t \geq 0$. Proof. We first notice that the solution to system (2.2) satisfies

$$S(t) = S(0)e^{-\int_0^t \beta(1 - u(s))I(s)ds} \tag{2.3}$$

$$I(t) = I(0)e^{\int_0^t (\beta(1 - u(s))S(s) - \gamma)ds} \tag{2.4}$$

$$R(t) = R(0) + \gamma \int_0^t I(s)ds \tag{2.5}$$

Therefore, $S(t), I(t) \geq 0$ for all $t \geq 0$ due to (2.3) and (2.4), respectively, where the latter further implies $R(t) \geq 0$ due to (2.5). Moreover, since $(S(t) + I(t) + R(t))' = 0$ for all t due to the dynamics (2.2), we know $S(t) + I(t) + R(t) = 1$ for all $t \geq 0$. Combining these facts, we conclude that $(S(t), I(t), R(t)) \in \Delta^2$ for all $t \geq 0$. $\square$

One can easily see that model (2.2) yields

$$\frac{dI}{dt} = \left(\frac{\beta}{\gamma}(1 - u(t))S(t) - 1\right)\gamma I(t), \tag{2.6}$$

where β/γ is the basic reproduction number. Clearly, if $\beta S(0)/\gamma < 1$, then the virus is contained (even though it can still benefit from mitigation measures that would further reduce the daily number of new infections). It also implies that an obvious way of controlling the disease, should $\beta S(0)/\gamma$ be greater than 1, is to choose $u(t)$ such that $0 < \beta S(t)(1 - u(t))/\gamma \ll 1$. That is, $1 > u(t) \gg 1 - \frac{\gamma}{S(t)\beta}$. However, all things considered, if the basic reproduction number, β/γ, is large, this kind of control may not be feasible. Indeed, while the right interventions at the onset of the disease save lives and protect the health of the population, they come with social, psychological, and economic costs. Therefore, policymakers have a difficult task of balancing the benefits to public health and the negative outcomes of their preventive measures. Mathematically, this comes down to solving the optimal control problem, where the main goal is to reduce the daily number of new infections, $\beta(1 - u(t))S(t)I(t)$, while also minimizing the cost of preventive measures, $\lambda c(u(t))$. This gives rise to the following objective functional:

$$J(\mathbf{x}, u) := \int_0^T \{(\beta(1 - u(t))S(t)I(t) + \lambda c(u(t))\} \, dt, \quad \lambda > 0.$$

According to (2.2), this $J(\mathbf{x}, u)$ can be written as

$$J(\mathbf{x}, u) = S(0) - S(T) + \lambda \int_0^T c(u(t)) \, dt, \quad \lambda > 0. \tag{2.7}$$

Evidently, the choice of the cost, $c(u(t))$, has a major impact on the resulting control strategy. It is important to define $c = c(u)$ and the corresponding Lagrangian, denoted below as $L(x, u; p, q)$, in such a way that the optimal solution, $u = u(t)$, is guaranteed to take values between 0 and 1. In other words, it should never be a feasible strategy for $u = u(t)$ to become negative, and the cost of control, $c(u(t))$, should get extremely high as $u(t)$ approaches 1 (unless the regularization parameter, λ, is very small).

For various epidemic models, a very common choice of $c(u(t))$ is $c(u(t)) = u^2(t)$ (Pal Bajiya et al., 2022; Tuncer et al., 2022), which is often implemented in conjunction with the forward−backward sweep numerical algorithm for the computation of optimal control $u = u(t)$ (Lenhart & Workman, 2007). However, as pointed out in (Pal Bajiya et al., 2022; Tuncer et al., 2022), there are some drawbacks of setting $c(u(t))$ to $u^2(t)$. Indeed, since this function has a finite penalty at $u(t) = 1$, an explicit constraint $u(t) \leq 1$ must be enforced. Without this constraint, it is easy to get $u(t) > 1$ (especially for small values of λ), which results in unrealistic strategy leading to $S'(t) > 0$. And even with the constraint $u(t) \leq 1$, the optimal control function often reaches the nonviable "ultimate" level, $u(t) = 1$, for the better part of the study period.

To avoid the above scenario, in our theoretical and numerical analysis, we consider $c = c(u)$ such that $\lim_{u \to 1^-} c(u) = \infty$. This important requirement, along with the assumption that the cost, $c = c(u)$, is twice continuously differentiable in its

domain containing $[0, 1)$, with $\frac{d^2c}{du^2} > 0$, $c(0) = 0$, $c'(u) > 0$ for $u \geq 0$, $c'(u) < 0$ for $u < 0$, allows us to design an optimal control problem leading to $u(t) < 1$ during the entire study period, $[0, T]$. For numerical simulations, we employ and compare 4 different cost functions for the optimal control strategy

$$c_1(u) = -\ln(1 - u^2), \ c_2(u) = -u\ln(1 - u), \ c_3(u) = -(u + \ln(1 - u)), \ \text{and} \ c_4(u) = u^2.$$

All these functions, except for $c_4(u)$, have infinite penalty at $u(t) = 1$, and the function $c_4(u) = u^2$ is used for comparison.

3. Properties of optimal control

In what follows, we prove our main theoretical result, Theorem 3.1, that has major practical implications. Namely, we show that beginning with some moment, $\tau \in [0, T)$, the optimal control strategy, $u = u(t)$, introduced in the previous section, is declining, which may cause the number of newly infected people to increase. So, the window from 0 to τ is the time for public health officials to prepare alternative mitigation measures, such as vaccines, testing, antiviral medications, and others.

Theorem 3.1. Assume that $u = u(t)$ is an optimal control trajectory for the objective functional (2.7) constrained by the system $\frac{d\mathbf{x}}{dt} = f(\mathbf{x}, u)$ defined in (2.2) and by the inequality $u(t) \geq 0$ for all $t \in [0, T]$. Let $c = c(u)$ be twice continuously differentiable in its domain containing $[0, 1)$, with $\frac{d^2c}{du^2} > 0$, $c(0) = 0$, $c'(u) > 0$ for $u \geq 0$, $c'(u) < 0$ for $u < 0$, and $\lim_{u \to 1^-} c(u) = \infty$. Then there is $\tau \in [0, T)$ such that for any $t \in [\tau, T]$, the derivative, $u'(t)$, exists and $u'(t) \leq 0$.

Proof. Without loss of generality, we assume $S(t), I(t) > 0$ (since otherwise it is clear that $u'(t) = 0$). Given the constraints $\frac{d\mathbf{x}}{dt} = f(\mathbf{x}, u)$ and $u(t) \geq 0$ for all $t \in [0, T]$, the optimal control problem results in the following Lagrangian

$$L(\mathbf{x}, u; p, q) = S(0) - S(T) + \int_0^T \{\lambda c(u(t)) - p(t) \cdot (\mathbf{x}'(t) - f(\mathbf{x}(t), u(t))) - q(t)u(t)\} dt \tag{3.1}$$
$$- p(0) \cdot (\mathbf{x}(0) - \mathbf{x}_0), \quad p(t) = [p_1(t), p_2(t), p_3(t)]^\top.$$

Then the Karush–Kuhn–Tucker (KKT) conditions are as follows

$(C1) \quad \lambda c'(u) + p \cdot \partial_u f(\mathbf{x}, u) - q = 0 \tag{3.2}$

$(C2) \quad p' = -\partial_x f(\mathbf{x}, u)^\top p, \quad p(T) = [-1, 0, 0]^\top \tag{3.3}$

$(C3) \quad \mathbf{x}' = f(\mathbf{x}, u), \quad \mathbf{x}(0) = \mathbf{x}_0 \tag{3.4}$

$(C4) \quad q(t) \geq 0, \quad u(t) \geq 0, \quad q(t)u(t) = 0, \quad \forall t \in [0, T]. \tag{3.5}$

From (C1) we conclude that $\lambda c'(u) - q = -p \cdot \partial_u f(\mathbf{x}, u) = -\beta SI(p_1 - p_2)$, which is differentiable and hence continuous since all terms on the right-hand side are so due to (C2) and (C3). Furthermore, since $p_1(T) = -1 < 0 = p_2(T)$ and $S(t), I(t) > 0$, there exist $\tau_1, \tau_2 \in [0, T)$ such that $p_1(t) < p_2(t)$ for all $t \in [\tau_1, T)$ and $p_1(t) < 0$ for all $t \in [\tau_2, T)$. Let $\tau = \max(\tau_1, \tau_2)$, then

$$p_1(t) < 0 \quad \text{and} \quad \lambda c'(u(t)) - q(t) = -\beta S(t)I(t)(p_1(t) - p_2(t)) > 0 \quad \forall t \in [\tau, T]. \tag{3.6}$$

Now we restrict our discussion to $[\tau, T]$. If $c'(u(t)) = 0$ for some t, then $u(t) = 0$ by the property of c, and hence $q(t) = \beta S(t)I(t)(p_1(t) - p_2(t)) < 0$ which contradicts to (C4). Therefore $c'(u(t)) > 0$ for all t by the assumptions on c and $0 < u(t) < 1$, where the latter also implies $q(t) = 0$ for all t due to (C4). In summary, over $[\tau, T]$, we have

$$\lambda c'(u(t)) + \beta S(t)I(t)(p_1(t) - p_2(t)) = 0.$$

Then by implicit function theorem we know u' exists and

$$u'(t) = -\frac{\beta[S(t)I(t)(p_1(t) - p_2(t))]'}{\lambda c''(u(t))} \quad \text{for all} \quad t \in [\tau, T]. \tag{3.7}$$

Taking into consideration (2.2) and (C2), for all $t \in [\tau, T]$, one has $p_3(t) = 0$ and

$$\begin{cases} \dot{p}_1 = -\beta(p_2 - p_1)(1 - u)I \\ \dot{p}_2 = -\beta(p_2 - p_1)(1 - u)S + \gamma p_2 \\ p_1(T) = -1, \ p_2(T) = 0. \end{cases} \tag{3.8}$$

From system (3.8), one concludes

$$\dot{p}_2 - \dot{p}_1 = \beta \,(p_2 - p_1)(1 - u)(I - S) + \gamma \,p_2. \tag{3.9}$$

Combining (2.2) and (3.9), one can rewrite $[S(t)I(t)(p_1(t) - p_2(t))]'$ as follows

$$
\begin{aligned}
[S(t)I(t)(p_1(t) - p_2(t))]' \quad &= \beta\,(p_2 - p_1)(1 - u)(I - S)SI + \gamma p_2 SI \\
&+ (p_2 - p_1)\Big\{ -\beta(1 - u)SI^2 + \beta(1 - u)S^2 I - \gamma SI \Big) \Big\} \\
&= \{\beta\,(p_2 - p_1)(1 - u)(I - S) + \gamma p_2 + \beta\,(p_2 - p_1) \\
&\quad \times (1 - u)(S - I) - \gamma(p_2 - p_1)\}SI = \gamma p_1 SI.
\end{aligned}
$$

According to (3.6) and (3.7), this yields for all $t \in [\tau, T]$,

$$u'(t) = -\frac{\beta[S(t)I(t)(p_1(t) - p_2(t))]'}{\lambda c''(u(t))} = \frac{\beta\gamma S(t)I(t)p_1(t)}{\lambda c''(u(t))} < 0. \tag{3.10}$$

This completes the proof. □

Remark 3.2. As it follows from (3.10), the impact of $u(t)$ scaling down towards the end of the early stage of the outbreak will depend on the weight, λ. If the wight on control is relatively high (see Figs. 3 and 4 in Section 5), then the decline in $u(t)$ for $t \geq \tau$ can be substantial, which will result in a notable surge in the daily number of infected individuals, $\mathcal{I}(t)$, for $t \geq \tau$. On the other hand, if the weight, λ, is small (as in Fig. 5), then by the time $t = \tau$ the epidemic is effectively contained. Hence the decline in $u(t)$ for $t \geq \tau$ is negligible and the daily number of infected people, $\mathcal{I}(t)$, remains very low for $t \geq \tau$.

Note that cost functional (2.7) aims to minimize the cumulative number of cases during the early phase of the disease, i.e., for $t \in [0, T]$. However, it does not guarantee that on any given day, the number of infected individuals in the optimally controlled environment is less than the number of infected individuals in the same environment but with no control. As our experiments below illustrate, when the weight on control, λ, is relatively high, towards the end of the study period in a controlled environment the daily number of infected humans, $\mathcal{I}(t)$, can potentially bypass the corresponding $\mathcal{I}(t)$ in the environment with no control (see Figs. 3 and 4 in Section 5).

The objective functional (2.7) is set to minimize the cumulative number of infections, $S(0) - S(T)$, while keeping the negative impact of mitigation measures at bay. This is achieved, for the most part, by reducing the daily number of new infections but also, apparently, by delaying some infections. On the bright side, $\mathcal{I}(t)$ in the controlled environments gets bigger than $\mathcal{I}(t)$ in the uncontrolled case only when t is approaching T. It is reasonable to assume that at this time additional intervention measures become available that will gradually replace the initial set of controls.

In the running cost, rather than minimizing the daily number of new infections, one can also minimize the daily number of infected individuals. This gives rise to the following objective functional

$$\tilde{J}(\mathbf{x}, u) := \int_0^T \{I(t) + \lambda \, c(u(t))\}\, dt = \frac{R(T) - R(0)}{\gamma} + \lambda \int_0^T c(u(t))\, dt. \tag{3.11}$$

That is, instead of maximizing $S(T)$, this functional aims to minimize $R(T)$. Using the similar argument as above, one can show that this optimal control strategy, $\tilde{u}(t)$, will also be decreasing starting with some point $\tilde{\tau} \in [0, T)$.

4. Numerical algorithm for learning control

To learn the optimal control function, $u : [0, T] \to \mathbb{R}$, which is guaranteed to take values in $[0, 1)$ according to Theorem 3.1 above, we employ a deep learning based numerical algorithm. This algorithm can be easily modified to the case of vector-valued controls. At the first step, we parameterize u as a deep neural network (DNN), denoted by u_θ, with parameters $\theta \in \mathbb{R}^m$. In our experiments, we chose a simple fully connected network with both input and output layer dimension 1 (because in our setting, the input is time $t \in [0, T]$ and the output is a scalar). We set u_θ to have 4 hidden layers and each layer is of size 10. Specifically, the function u_θ is defined by

$$u_\theta(t) = w_5^\top \sigma(W_4 z_4 + b_4) + b_5, \quad \text{where} \quad z_{l+1} = \sigma(W_l z_l + b_l) \quad \text{for} \quad l = 0, 1, 2, 3$$

and $z_0 := t \in \mathbb{R}$. Here $\sigma(z) := \tanh(z)$ is the activation function that applies to the argument componentwise, and $\theta = (w_5, W_4, W_3, W_2, W_1, W_0, b_5, b_4, b_3, b_2, b_1, b_0)$ is a column vector that contains all the components of these variables, where $w_5 \in \mathbb{R}^{10}$, W_4, $W_3, W_2, W_1 \in \mathbb{R}^{10\times 10}$, $W_0 \in \mathbb{R}^{10\times 1}$, $b_5 \in \mathbb{R}$, $b_4, b_3, b_2, b_1, b_0 \in \mathbb{R}^{10}$, and all vectors are considered as column vectors. The number m is the dimension of θ (i.e., the total number of components in θ), which is $m = 471$ in our case. Introduce the notation $\ell(\theta) := J(\mathbf{x}, u_\theta)$, where J is defined in (2.7) and $\mathbf{x}$ follows the dynamics (2.2) with the given initial state $\mathbf{x}(0) = (S(0), I(0), R(0))$. To find the optimal u_θ, we essentially need to compute $\nabla_\theta \ell(\theta)$ for any θ and apply the gradient descent to update θ. In our algorithm, we employ the neural ordinary differential equation (NODE) method (Chen, Rubanova, Bettencourt, & Duvenaud, 2018) which computes $\nabla_\theta \ell(\theta)$ in the following way. First, with the given θ, one solves the ODE forward in time:

$$\dot{\mathbf{x}}(t) = f(\mathbf{x}(t), u_\theta(t)), \quad t \in [0, T], \tag{4.1}$$

with initial value $\mathbf{x}(0) = \mathbf{x}_0$ and $f(\mathbf{x}, u)$ defined in (2.2). Second, one solves the augmented adjoint equation backward in time:

$$(\dot{\mathbf{p}}(t), \ \dot{\mathbf{a}}(t)) = -(\mathbf{p}(t) \partial_{\mathbf{x}} f(\mathbf{x}(t), u_\theta(t)), \ \mathbf{p}(t) \partial_u f(\mathbf{x}(t), u_\theta(t)) \partial_\theta u_\theta(t)), \quad t \in [0, T], \tag{4.2}$$

with terminal value $(\mathbf{p}(T), \mathbf{x}(T)) = (-\nabla h(\mathbf{x}(T)), \mathbf{0})$. Here $\mathbf{x}, \mathbf{p}, \mathbf{a}$ are all row vectors at each time t. Then it can be shown that $\nabla_\theta \ell(\theta) = \mathbf{a}(0)$ (Chen et al., 2018). The algorithm is summarized in Algorithm 1 below. The implementation, training and testing were conducted in Python 3.9.6 with PyTorch 2.1.0 and Torchdiffeq 0.2.3. We initialize the parameter θ using Xavier initialization built in the PyTorch package.

Algorithm 1. Neural ODE method to solve the optimal control problem of u

---
Require: Cost function c and weight $\lambda > 0$. Network structure u_θ. Initial guess θ.
Ensure: Optimal control u_θ with trained θ.
  repeat
    Solve $\mathbf{x}$ forward in time using (4.1).
    Solve $(\mathbf{p}, \mathbf{a})$ backward in time using (4.2).
    $\theta \leftarrow \theta - \mu \mathbf{a}(0)$.
  until converged.

A few details about the performance of Algorithm 1 and our numerical simulations.

- In our experiments, we try 4 different cost functions, $c = c(u)$. Details and discussion will be given in Section 5;
- The weight, λ, scales the cost function, $c = c(u)$, and can be critical to the optimal control solution. In Section 5, we conduct empirical study on different values of λ;
- One can apply any numerical integrator (e.g., Euler, mid-point, Runge-Kutta) to solve (4.1) and (4.2). We used the 4th order Runge-Kutta method (rk4) built in the PyTorch package;
- One can either solve $(\mathbf{p}, \mathbf{a})$ as in (4.2) or solve $\mathbf{x}$ jointly backward in time to avoid saving $\mathbf{x}(t)$ obtained forward in (4.1) in the memory;
- In Algorithm 1, one can choose the step size $\mu > 0$ and terminate the algorithm after a prescribed number of iterations, K. We used Adam (Kingma et al., 2015) with deterministic gradient and set these parameters as $\mu = 0.001$ and $K = 1,000$ and other parameters as default. The results appear to be stable for values around them;
- Since the control problem is not convex in $(\mathbf{x}, u)$, it is not guaranteed that our solution is the global minimizer. This is, unfortunately, a common issue in solving optimal control problems. Nevertheless, in all experiments, the numerical solutions obtained by our method appear to satisfy the constraint $u(t) \in [0, 1)$ for all $t \in [0, T]$ and $du(t)/dt < 0$ starting with some $\tau \in [0, T)$;
- In the above Algorithm, we followed the idea of neural ODE (Chen et al., 2018) and set $\mathbf{a}(t)$ to be the auxiliary variable in order to compute the gradient of the loss function $\ell(\theta)$ with respect to θ. Specifically, by solving the augmented adjoint dynamics (4.2) backward in time, one can show that $\mathbf{a}(0) = \nabla_\theta \ell(\theta)$, which allows to find the (local) minimizer of the loss function $\ell(\theta)$ by the gradient descent method. More details about the derivation can be found in (Chen et al., 2018).

5. Numerical results and discussion

In this section, we apply the deep learning based numerical algorithm to solve the optimal control problem (2.7) subject to SIR model (2.2) with the following four cost functions:

$$\begin{aligned}
c_1(u) &= -0.830071 \ln(1 - u^2) \\
c_2(u) &= -0.672850\, u \ln(1 - u) \\
c_3(u) &= -u - \ln(1 - u) \\
c_4(u) &= 1.424546\, u^2.
\end{aligned}$$

The weight 0.830071 in c_1 is chosen to minimize the distance

$$\int_0^1 w(z) |c_1(z) - c_3(z)|^2 \, dz, \quad w(z) = \sqrt{1 - z^2},$$

(the same for c_2, c_4). Doing so makes c_i's close in the w-weighted 2-norm sense. See the comparison of these cost functions in Fig. 1.
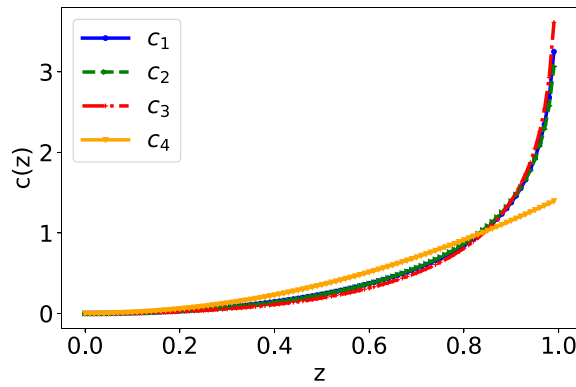
Fig. 1. Comparison of different cost functions c.

In our experiments, we consider λ as 0.1, 0.05, 0.01, and 10^{-7}. For $\lambda = 0.1$, the environment is close to no control as shown in Fig. 2, since the penalty on control is weighted highly. All values of λ larger than 0.1 resulted in a similar behavior and hence they were omitted here.

As λ gradually decreases, we see that controls start to make impact as they become cheaper to implement. For example, as shown in Fig. 3, when $\lambda = 0.05$, we observe that $c_1(u)$, $c_2(u)$, and $c_3(u)$ generate similar control strategies that effectively suppress the cumulative number of infected people (or equivalently maximize $S(T)$).

We note that all three controls, $c_1(u)$, $c_2(u)$, and $c_3(u)$, make a considerable positive impact on how the epidemic unfolds. Even though $\mathcal{I}(t)$ in the controlled environment is still growing (see Table 1), the daily number of infected people remains low for a long time. However, as expected from our theoretical analysis, for all three cost functions, $c_1(u)$, $c_2(u)$, and $c_3(u)$, and $\lambda = 0.05$, the corresponding control strategies, $u(t)$, begin to decrease after some point.

Thus, towards the end of the study period in a controlled environment the daily number of infected humans, $\mathcal{I}(t)$, bypasses the corresponding $\mathcal{I}(t)$ in the environment with no control.

As mention in Remark 3.4, the objective functional (2.7) is set to minimize the cumulative number of infections, $\mathcal{S}(0) - \mathcal{S}(T)$, which it does successfully as it is evident from Table 2. This is achieved, for the most part, by reducing the daily number of new infections but also, apparently, by delaying some infections.

As one can clearly see from Fig. 3 and Tables 1 and 2, the cost of the optimal control strategy, $u(t)$, corresponding to c_4, is still very high for $\lambda = 0.05$, and this control does not defeat the outbreak. The reason for this control being different from $c_1(u)$, $c_2(u)$, and $c_3(u)$ can be understood from Fig. 1, which shows that the cost, $c_4(u)$, is greater than the cost of all other controls between $u = 0.2$ and $u = 0.8$.
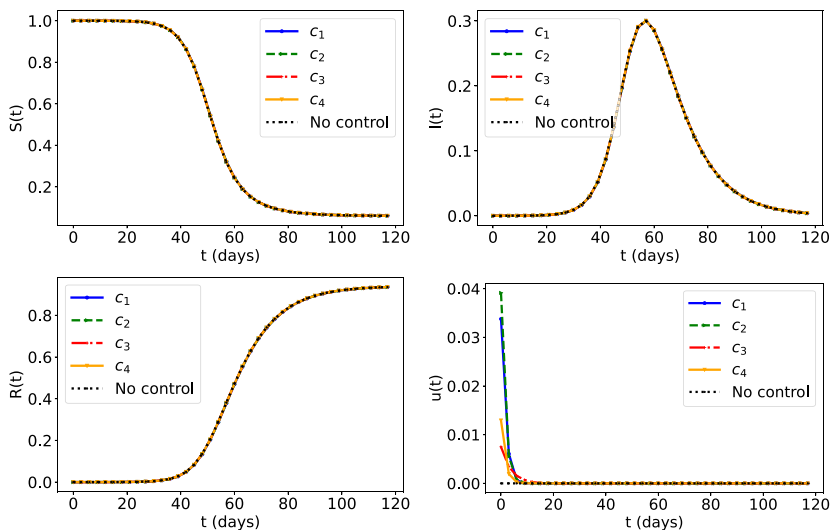
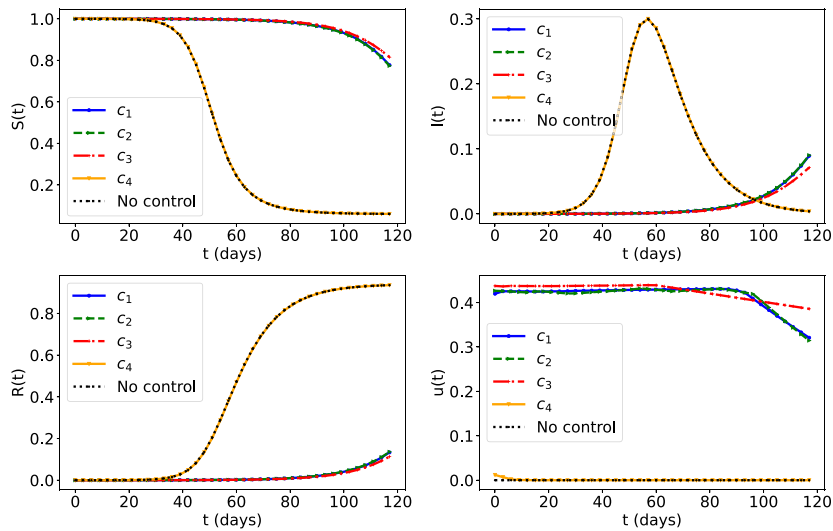

Fig. 2. Weight $\lambda = 0.1$.

Fig. 3. Weight $\lambda = 0.05$.

When λ reaches 0.01, the scale on the cost function is small and all optimal control strategies, $u(t)$, corresponding to cost functions $c_1(u)$, $c_2(u)$, $c_3(u)$, and $c_4(u)$ appear to suppress infections more aggressively, as illustrated in Fig. 4. The actual values of $\mathcal{I}(t)$ are shown in Table 3. The total numbers of infected people up to day t, $\mathcal{S}(0) - \mathcal{S}(t)$, for all four control functions, $c_1(u)$, $c_2(u)$, $c_3(u)$, and $c_4(u)$, are presented in Table 4.

As λ continues to decrease, we see similar behavior as in Fig. 4 except that $u(t)$ become larger and the infections are further suppressed. For example, when $\lambda = 10^{-7}$, the cost is very lightly weighted and hence one can impose greater control as shown in Fig. 5.

Again, the behavior of $c_4(u)$ is different. As mentioned above, this control requires an explicit constraint, $u(t) \in [0, 1]$. If not, it is easy to get $u(t) > 1$ (especially for small λ), which is not realistic because it makes $S'(t) > 0$. With the constraint enforced, $u(t)$, corresponding to $c_4(u)$, is likely slipping into a local minimum.

As illustrated in Fig. 5, by the time $u(t)$ begins to decrease, the epidemic is effectively under control. Hence, as it follows from (3.10), the decline in $u(t)$ for $t \geq \tau$ is negligible and the daily number of infected people, $\mathcal{I}(t)$, remains very low for $t \geq \tau$.

For all numerical experiments presented in this section, we let the entire population, N be 10^7 people with $\mathcal{I}(0) = 200$, $\mathcal{R}(0) = 0$, and $\mathcal{S}(0) = N - 200$.
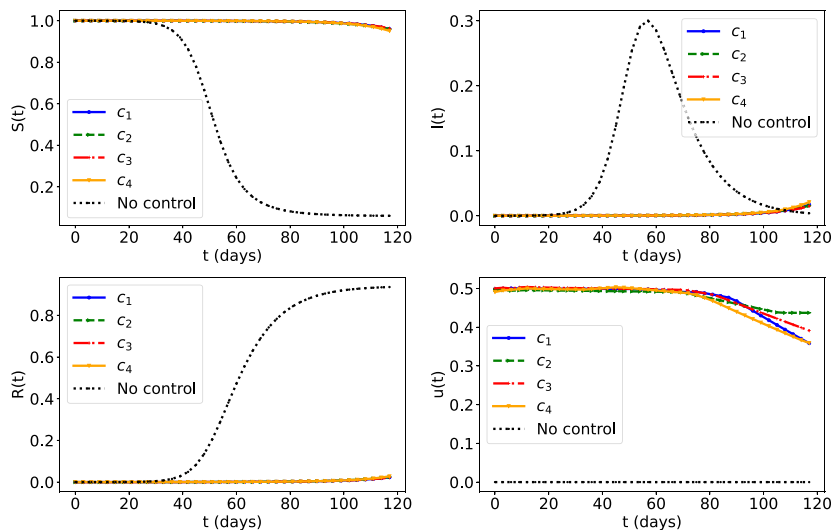

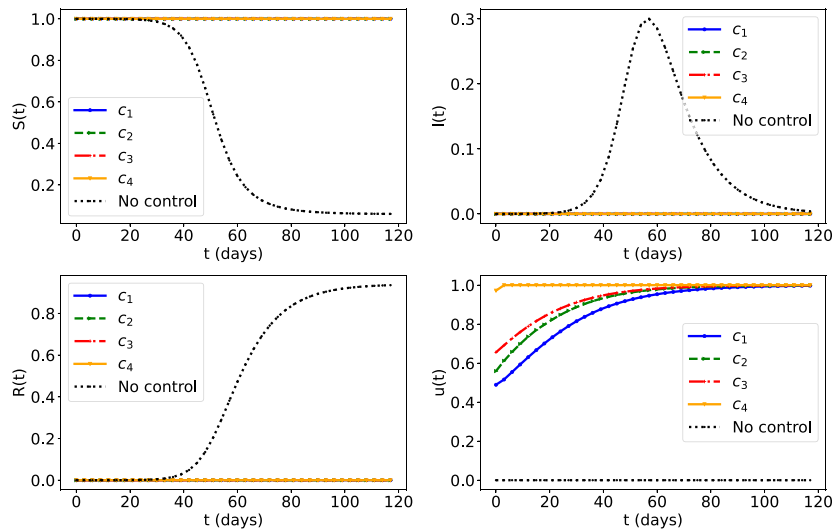
Fig. 4. Weight $\lambda = 0.01$.

Fig. 5. Weight $\lambda = 10^{-7}$.

Table 1
Number of infected people $\mathcal{I}(t)$ versus day t for $\lambda = 0.05$

Day	No control	c_1	c_2	c_3	c_4
0	200	200	200	200	200
10	1626	423	423	407	1600
20	12542	889	891	824	12341
30	92164	1856	1882	1660	90714
40	643531	3898	4004	3370	634826
50	2358721	8104	8348	6785	2344806
60	2852657	16674	17093	13546	2858895
70	1722500	34405	35574	27592	1731405
80	834814	69687	72449	57021	839919
90	373748	137590	143188	118394	376160
100	164980	276638	282921	245423	166065
110	71628	567049	572008	479114	72103

We use $T = 120$, which mimics a 4-months time frame. This value of T allows us to realistically assume that individuals recovered from COVID-19 still have immunity and stay in the removed class, $\mathcal{R}$, for the entire duration of the study period. Furthermore, we take $\beta = 0.3$ and $\gamma = 0.1$ days^{-1}, which correspond to the reproduction number, $\mathfrak{R} = 3$, and the recovery rate of 10 days.

Table 2
Total number of infected people up to day t, $N - \mathcal{S}(t)$, for $\lambda = 0.05$

Day	No control	c_1	c_2	c_3	c_4
0	200	200	200	200	200
10	2339	734	731	709	2303
20	18723	1835	1843	1724	18425
30	138618	4154	4182	3786	136445
40	993903	9034	9212	7991	980029
50	4179153	19132	19626	16404	4146211
60	7574716	39793	40813	33135	7557842
70	8800810	82846	85337	67540	8795738
80	9181982	169453	175482	138477	9180310
90	9316270	339228	352155	285376	9315647
100	9367572	682997	703593	592907	9367317
110	9388987	1389004	1413628	1187340	9388880

Table 3
Number of infected people $\mathcal{I}(t)$ versus day t for $\lambda = 0.01$

Day	No control	c_1	c_2	c_3	c_4
0	200	200	200	200	200
10	1626	335	340	333	339
20	12542	559	575	550	567
30	92164	932	973	912	951
40	643531	1563	1660	1522	1599
50	2358721	2616	2829	2542	2649
60	2852657	4380	4818	4245	4431
70	1722500	7447	8269	7155	7587
80	834814	12778	14502	12221	13336
90	373748	22520	26401	21821	25197
100	164980	43921	50317	42319	52546
110	71628	95049	97855	87251	117329

Table 4
Total number of infected people up to day t, $N - \mathcal{S}(t)$, for $\lambda = 0.01$

Day	No control	c_1	c_2	c_3	c_4
0	200	200	200	200	200
10	2339	604	612	600	615
20	18723	1276	1304	1261	1289
30	138618	2394	2474	2358	2437
40	993903	4287	4485	4189	4369
50	4179153	7424	7899	7250	7554
60	7574716	12685	13704	12335	12865
70	8800810	21705	23742	20996	22079
80	9181982	37149	41310	35740	38214
90	9316270	64362	73392	62132	68915
100	9367572	118524	135484	114391	134473
110	9388987	236989	256274	222679	281497

6. Conclusions

In our study, we combine theoretical analysis with rigorous numerical exploration of an optimal control problem for the early stage of an infectious disease outbreak. We design an objective functional aimed at minimizing the cumulative number of cases. The running cost of control, satisfying mild, problem-specific, conditions generates an optimal control tragectory, $u(t)$, that stays inside its admissible set for any $t \in [0, T]$. For the optimal control problem, restricted by SIR compartmental model (Susceptible $\rightarrow$ Infectious $\rightarrow$ Removed) of disease transmission, we show that the optimal control strategy, $u(t)$, may be growing until some moment $\tau \in [0, T]$. However, for any $t \in [\tau, T]$, the derivative, $\frac{du}{dt}$, becomes negative and $u(t)$ declines as t approaches T possibly causing the number of newly infected people to go up. So, the window from 0 to τ is the time for public health officials to prepare alternative mitigation measures, such as vaccines, testing, and antiviral medications, and to plan for the deployment of rescue equipments like ventilators and beds.

The impact of $u(t)$ decreasing towards the end of the early stage depends on the weight, λ. If λ is relatively large, then the decline in $u(t)$ for $t \geq t$ may be significant, which can result in a considerable surge in the daily number of infected individuals, $\mathcal{I}(t)$, for $t \geq \tau$. On the other hand, if λ is small, then by the time $t = \tau$ the epidemic is effectively under control. Hence, as it follows from (3.10), the decline in $u(t)$ for $t \geq \tau$ is negligible and the daily number of infected people, $\mathcal{I}(t)$, remains very low for $t \geq \tau$.

Our theoretical findings are illustrated with important numerical examples showing optimal control strategies for various cost functions and weights. Simulation results provide a comprehensive demonstration of the effects of control on the epidemic spread and mitigation expenses, which can serve as invaluable references for public health officials. The important next step is to consider the case of vector-valued controls that, on top of early non-medical interventions (such as social distancing, restrictions on travel and mass gatherings, isolation and quarantine of confirmed cases), include treatment with antivirals and the optimal vaccination strategy.

CRediT authorship contribution statement

Alexandra Smirnova: Writing − original draft, Methodology, Investigation, Formal analysis, Conceptualization. **Xiaojing Ye:** Writing − review & editing, Validation, Software, Methodology, Investigation, Formal analysis.

Declaration of Competing Interest

No conflict.

Acknowledgement

We would like to thank Nathan Gaby for providing assistance to the initial implementation of the code. We would also like to express our deepest gratitude to the associate editor and to the reviewers for their most valuable comments on our manuscript.

References

CDC Center for Disease Control and Prevention. (2023a). _People with certain medical conditions_.

CDC Center for Disease Control and Prevention. (2023b). _Understanding risk_.

Chen, R. T. Q., Rubanova, Y., Bettencourt, J., & Duvenaud, D. K. (2018). Neural ordinary differential equations. _Advances in Neural Information Processing Systems, 31_.

David Paltiel, A., Zheng, A., & Walensky, R. P. (2020). Assessment of sars-cov-2 screening strategies to permit the safe reopening of college campuses in the United States. _JAMA Network Open, 3_(7), Article e2016818.

Drugs.com. (2022). _How do covid-19 symptoms progress and what causes death?_.

Dutta, P., Samanta, G. P., & Nieto, J. J. (2024). Periodic transmission and vaccination effects in epidemic dynamics: A study using the sivis model. _Nonlinear Dynamics, 112_, 2381–2409.

Hadi, M. A., & Ali, H. I. (2020). Control of covid-19 system using a novel nonlinear robust control algorithm. _Biomedical Signal Processing and Control_, 102.

HHS U.S. Department of Health and Human Services. (2023). _What are the possible treatment options for covid-19?_.

Igoe, M., Casagrandi, R., Gatto, M., Hoover, C. M., Mari, L., Ngonghala, C. N., et al. (2023). Reframing optimal control problems for infectious disease management in low-income countries. _Bulletin of Mathematical Biology, 85_(4:31).

Kingma, D. P., & Adam, J. B. (2015). A method for stochastic optimization. In Y. Bengio, & Y. LeCun (Eds.), _3rd International conference on learning representations, ICLR 2015, San Diego, CA, USA, may 7-9, 2015, conference track proceedings_.

Kudryashov, N. A., Chmykhov, M. A., & Vigdorowitsch, M. (2021). Analytical features of the sir model and their applications to covid-19. _Applied Mathematical Modelling, 90_, 466–473.

Lee, S., Chowell, G., & Castillo-Chávez, C. (2010). Optimal control for pandemic influenza: The role of limited antiviral treatment and isolation. _Journal of Theoretical Biology, 265_(2), 136–150.

Lenhart, S., & Workman, J. T. (2007). _Optimal control applied to biological models_. Chapman and Hall/CRC.

Li, L., Yang, Z., Dang, Z., Meng, C., Huang, J., Meng, H., et al. (2020). Propagation analysis and prediction of the COVID-19. _Infectious Disease Modelling, 5_, 282–292.

Lloyd-Smith, J. O., Schreiber, S. J., Kopp, P. E., & Getz, W. M. (2005). Superspreading and the effect of individual variation on disease emergence. _Nature, 438_, 355–359.

Locatelli, I., Trächsel, B., & Rousson, V. (2021). Estimating the basic reproduction number for covid-19 in western europe. _PLoS One, 16_(3), Article e0248731.

Marshall, N., Barlow, M., & Tyson, R. (2021). Optimal shutdown strategies for covid-19 with economic and mortality costs: British columbia as a case study. _Royal Society Open Science, 8_, 1–18.

O'Driscoll, M., Ribeiro Dos Santos, G., Wang, L., Cummings, D. A. T., Azman, A. S., Paireau, J., et al. (2021). Age-specific mortality and immunity patterns of sars-cov-2. _Nature, 590_, 140–145.

Ogilvy Kermack, W., & McKendrick, A. G. (1927). A contribution to the mathematical theory of epidemics. _Proceedings of the Royal Society of London - Series A: Containing Papers of a Mathematical and Physical Character, 115_(772), 700–721.

Organisation for Economic Co-operation and Development. (2023). _Oecd policy responses to coronavirus (covid-19) flattening the covid-19 peak: Containment and mitigation policies_.

Pal Bajiya, V., Bugalia, S., Tripathi, J. P., & Martcheva, M. (2022). Deciphering the transmission dynamics of covid-19 in India: Optimal control and cost effective analysis. _Journal of Biological Dynamics, 16_(1), 665–712.

Panovska-Griffiths, J., Kerr, C. C., Stuart, R. M., Mistry, D., Klein, D. J., Viner, R. M., et al. (2020). Determining the optimal strategy for reopening schools, the impact of test and trace interventions, and the risk of occurrence of a second covid-19 epidemic wave in the UK: A modelling study. _The Lancet Child & Adolescent Health, 4_(11), 817–827.

Pazos, F. A., & Felicioni, F. (2020). _A control approach to the covid-19 disease using a seihrd dynamical model_. medRxiv.

Pei, Y., Aruffo, E., Gatov, E., Tan, Y., Qi, L., Ogden, N., et al. (2022). School and community reopening during the covid-19 pandemic: A mathematical modelling study. _Royal Society Open Science, 9_(2), Article 211883.

Perkins, T. A., & España, G. (2020). Optimal control of the covid-19 pandemic with non-pharmaceutical interventions. _Bulletin of Mathematical Biology, 82_(9), 118.

Radin, J. M., Quer, G., Ramos, E., Baca-Motes, K., Gadaleta, M., Topol, E. J., et al. (2021). Assessment of prolonged physiological and behavioral changes associated with covid-19 infection. −e2115959, 07 _JAMA Network Open, 4_(7), Article e2115959.

Saha, S., & Samanta, G. P. (2021). Modelling the role of optimal social distancing on disease prevalence of covid-19 epidemic. _International Journal of Dynamics and Control, 9_, 1053–1077.

Saha, S., & Samanta, G. P. (2022). Analysis of a host–vector dynamics of a dengue disease model with optimal vector control strategy. _Mathematics and Computers in Simulation, 195_, 31–55.

Saha, S., Samanta, G. P., & Nieto, J. J. (2018). Stability analysis and optimal control of avian influenza virus a with time delays. _International Journal of Dynamics and Control, 6_(3), 1351–1366.

Saha, S., Samanta, G. P., & Nieto, J. J. (2020). Epidemic model of covid-19 outbreak by inducing behavioural response in population. _Nonlinear Dynamics, 102_, 455–487.

Saha, S., Samanta, G. P., & Nieto, J. J. (2022). Impact of optimal vaccination and social distancing on covid-19 pandemic. _Mathematics and Computers in Simulation, 200_, 285–314.

Samanta, G. P., & Gómez Aíza, R. (2015). Analysis of a delayed epidemic model of diseases through droplet infection and direct contact with pulse vaccination. _International Journal of Dynamics and Control, 3_, 275–287.

Soledad Aronna, M., Guglielmi, R., & Moschen, L. M. (2020). _A model for covid-19 with isolation, quarantine and testing as control measures_.

Summer, A., Aghaee, M., Martcheva, M., & Hager, W. (2023). Solving singular control problems in mathematical biology using pasa. _Computational and Mathematical Population Dynamics, 16_(1), 412–438.

Svoboda, J., Tkadlec, J., Pavlogiannis, A., Chatterjee, K., & Nowak, M. A. (2022). Infection dynamics of covid-19 virus under lockdown and reopening. _Scientific Reports, 12_(1), 1–11.

Szendroi, B., & Csanyi, G. (2004). Polynomial epidemics and clustering in contact networks. _Proceedings of the Royal Society of London. Series B: Biological Sciences, 5_, 364–366.

Tang, B., Wang, X., Li, Q., Bragazzi, N. L., Tang, S., Xiao, Y., et al. (2020). Estimation of the transmission risk of the 2019-nCoV and its implication for public health interventions. *Journal of Clinical Medicine, 9*(2).

Tuncer, N., Timsina, A., Nuno, M., Chowell, G., & Martcheva, M. (2022). Parameter identifiability and optimal control of a sars-cov-2 model early in the pandemic. *Journal of Biological Dynamics, 16*(1), 412—438.

Vincent, D., Bruyère, O., Louppe, G., Bureau, F., D'orio, V., Fontaine, S., et al. (2022). Decision-based interactive model to determine re-opening conditions of a large university campus in Belgium during the first covid-19 wave. *Archives of Public Health, 80*(1), 1—13.

Weiss, R. A., & McMichael, A. J. (2004). Social and environmental risk factors in the emergence of infectious diseases. *Nature Medicine, 10*(12), 70—76.

WHO World Health Organization. (2023). *Who coronavirus (covid-19) dashboard*.

Zhao, S., Lin, Q., Ran, J., Musa, S. S., Yang, G., Wang, W., et al. (2020). Preliminary estimation of the basic reproduction number of novel coronavirus (2019-ncov) in China, from 2019 to 2020: A data-driven analysis in the early phase of the outbreak. *International Journal of Infectious Diseases, 92*, 214—217.